JOC The Journal of Organic Chemistry

Article

pubs.acs.org/joc

Mechanistic Study of the Selectivity of Olefin versus Cyclobutene Formation by Palladium(0)-Catalyzed Intramolecular C(sp^3)–H Activation

Christos E. Kefalidis,[†] Michaël Davi,[‡] Philipp M. Holstein,[‡] Eric Clot,*[,†] and Olivier Baudoin*[,‡]

[†]Institut Charles Gerhardt, CNRS UMR 5253, Université Montpellier 2, case courrier 1501, Place Eugène Bataillon, 34095 Montpellier, France

[‡]Université Claude Bernard Lyon 1, CNRS UMR 5246 - Institut de Chimie et Biochimie Moléculaires et Supramoléculaires, CPE Lyon, 43 Boulevard du 11 Novembre 1918, 69622 Villeurbanne, France

Supporting Information

ABSTRACT: This study describes the mechanism and selectivity pattern of the Pd^0-catalyzed C(sp^3)–H activation of a prototypical substrate bearing two linear alkyl groups. Experimentally, the use of the Pd/P(*t*-Bu)$_3$ catalytic system leads to a ca. 7:3 mixture of olefin and benzocyclobutene (BCB) products. The C–H activation step was computed to be favored for the secondary position α to the benzylic carbon over the primary position β to the benzylic carbon by more than 4 kcal mol^{-1}, in line with previous selectivity trends on analogous substrates. The five-membered palladacycle obtained through this activation step may then follow two different pathways, which were computationally characterized: (1) decoordination of the protonated base and reductive elimination to give the BCB product and (2) proton transfer to the aryl ligand and base-mediated β-H elimination to give the olefin product. Experiments conducted with deuterated substrates were in accordance with this mechanism. The difference between the highest activation barriers in the two pathways was computed to be 1.2 kcal mol^{-1} in favor of BCB formation. However, the use of a kinetic model revealed the critical influence of the kinetics of dissociation of HCO_3^- formed after the C–H activation step in actually directing the reaction toward either of the two pathways.

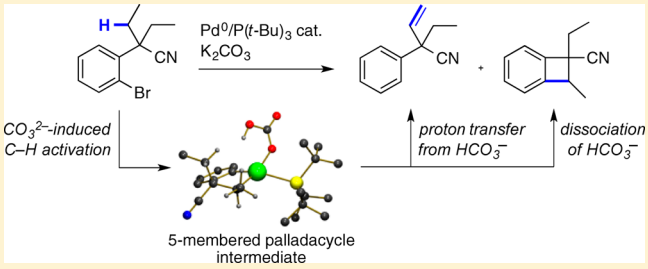

INTRODUCTION

Transition-metal-catalyzed C–H bond functionalization has recently emerged as a powerful tool to transform otherwise unreactive C–H bonds into carbon–carbon or carbon–heteroatom bonds.[1,2] This area is gradually changing the way chemists functionalize organic molecules by providing atom- and step-economical alternatives to more traditional methods and facilitating the access to valuable and original compounds. In contrast to the wealth of methods recently developed for the functionalization of arene and heteroarene C(sp^2)–H bonds,[3] relatively little work has focused on the functionalization of unreactive, nonacidic C(sp^3)–H bonds of alkyl groups.[4] In this context, our group[5] as well as others[6] have developed a series of palladium(0)-catalyzed reactions from aryl halides or pseudo-halides for the construction of C(sp^3)–C(sp^2) bonds or the dehydrogenation of C(sp^3)–C(sp^3) bonds based on C(sp^3)–H activation. These methods allow for the rapid and efficient synthesis of original structural motifs such as olefins, fused carbocycles and heterocycles, and polyarylated molecules.

In previous papers, we have computationally characterized the mechanism of the palladium(0)-catalyzed intramolecular C(sp^3)–H arylation of aryl halides **1** to give benzocyclobutenes (BCBs) **2**[5d,7] and indanes **3**[5f] (Scheme 1). These fused carbocycles arise from a sequence of five elementary steps starting with oxidative addition to an active palladium(0) species, followed by substitution of the halide with the carbonate base, base-assisted intramolecular C(sp^3)–H activation giving rise to a five- or six-membered palladacycle (**6**–**7**), decoordination of the protonated base, and reductive elimination. The formation of olefins **4** through C–H activation of linear alkyl groups, reported initially by us[5a−c] and subsequently by other groups,[6g,q] constitutes the missing link in this global mechanistic picture. The aim of the current mechanistic study is to fill this gap.

RESULTS AND DISCUSSION

Experimental Observations. We first analyzed the reaction of model substrate **1a** under standard conditions involving Pd(OAc)$_2$/P(*t*-Bu)$_3$ as the catalyst (10 mol % Pd), K_2CO_3 as the base (1.3 equiv), and DMF as the solvent (Scheme 2a). GC–MS analysis of the crude mixture revealed the formation of two sets of products in a 7:3 ratio, i.e., olefin **4a**, the identity of which was proven after chromatographic purification, and two other products of the same molecular

Special Issue: Mechanisms in Metal-Based Organic Chemistry

Received: July 17, 2014
Published: September 4, 2014

Scheme 1. Overall Mechanism for the Palladium(0)-Catalyzed C(sp^3)−H Activation of Aryl Halides

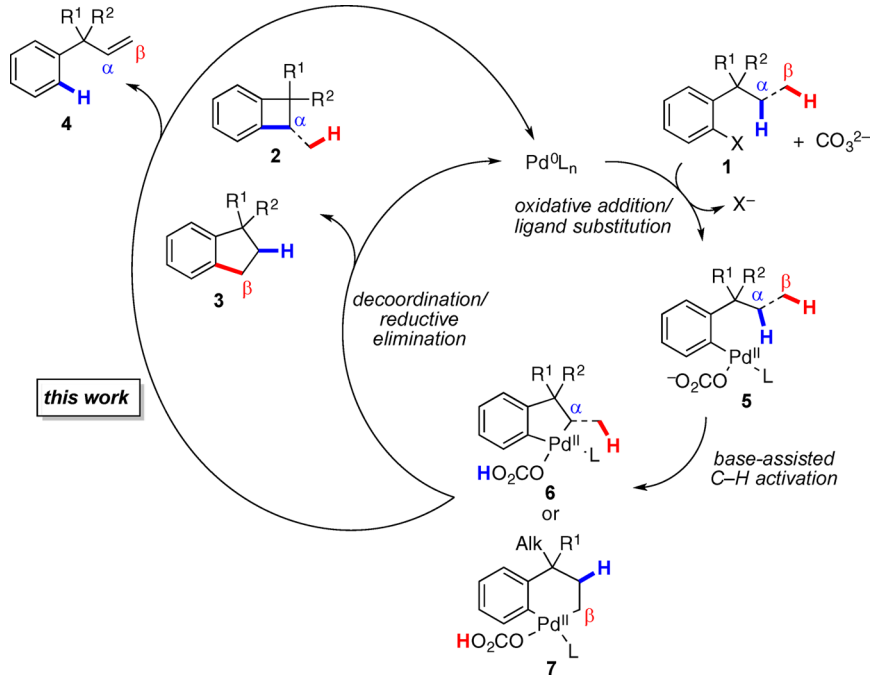

Scheme 2. C−H Activation of Protiated and Deuterated Substrates

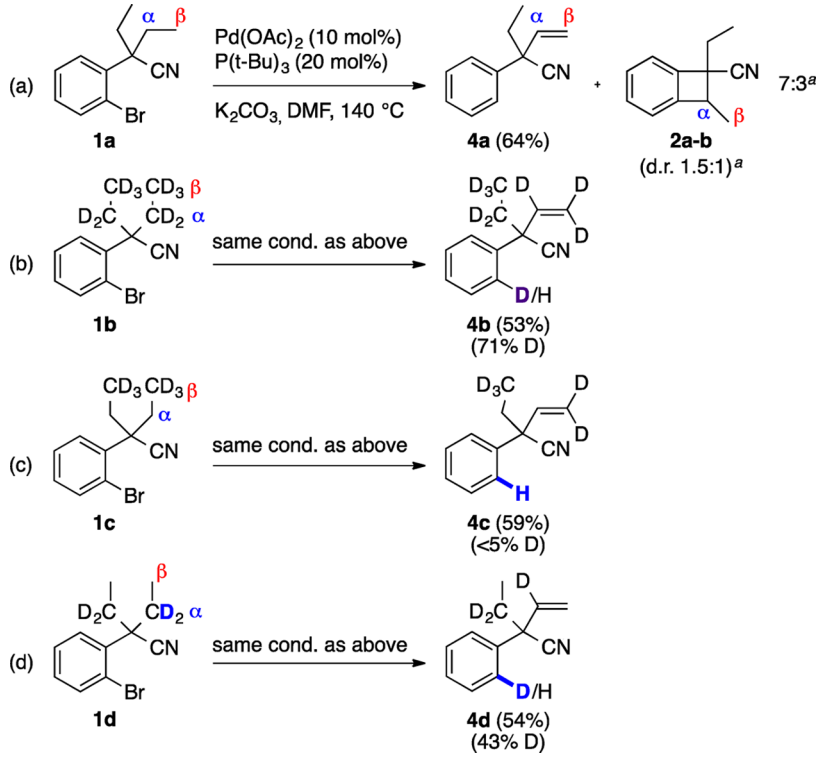

[a]GC ratio.

weight as **4a** (m/z 171 for [$M^{+\bullet}$]), tentatively assigned as BCB diastereoisomers **2a** and **2b** (d.r. = 1.5:1), which could not be isolated and unambiguously identified.[8] A similar product distribution was obtained with Pd_2dba_3 as the Pd source (10 mol % Pd) instead of $Pd(OAc)_2$, again with K_2CO_3 as the base. In contrast, with Pd_2dba_3 as the Pd source and KOAc instead of K_2CO_3, olefin **4a** was the only observed product. These results indicate that carbonate and not acetate is the active base when $Pd(OAc)_2$ is employed as the Pd source, in line with previous cases where a polar solvent such as DMF was employed.[5] Of note, the formation of **2a** and **2b** was not observed under previously reported conditions using P(*o*-tol)$_3$ or analogues[5a,b] and is currently favored by the use of P(*t*-Bu)$_3$, an optimal ligand for BCB formation.[5d] Although the formation of **2a** and

dx.doi.org/10.1021/jo501610x | J. Org. Chem. 2014, 79, 11903−11910

2b clearly arises from activation at one of the α C−H bonds of **1a**, it was not possible to conclude at this point whether the same initial bond cleavage is also responsible for the formation of olefin **4a**. To lift this ambiguity, the reactions of deuterated substrates **1b−d** were analyzed. First, the reaction of compound **1b** bearing fully deuterated ethyl groups was studied (Scheme 2b). Major albeit incomplete (71%) deuterium incorporation on the aromatic ring was observed by ^{2}H NMR spectroscopy (Figure S2 in the Supporting Information). This incomplete deuterium transfer can be assigned to an external proton source (presumably traces of water) exchanging with the migrating deuterium atom, consistent with previous observations on related Pd migrations.[9] Indeed, when nondeuterated substrate **1a** was reacted in the presence of 10 equiv of D_2O, partial deuterium incorporation on the aromatic ring was observed by ^{2}H NMR spectroscopy. The reaction of partially deuterated substrates **1c** and **1d** was next examined (Scheme 2c,d). Only product **4d** (but not **4c**) displayed deuterium incorporation on the aromatic ring as a result of H/D atom transfer from the α methylene carbon to the *ortho* sp^2 carbon. This observation is consistent with previous deuterium-labeling experiments[5a] and with the revised mechanism described in the next paragraph.

Computational Studies. Previous DFT calculations on the mechanism of the formation of BCB **2** from aryl halides (Scheme 1) catalyzed by Pd[P(*t*-Bu)$_3$] and mediated by CO_3^{2-} have already outlined the important features of this transformation.[5d,7] In particular, the crucial transition state (TS) associated with C−H activation presents a geometry where P(*t*-Bu)$_3$ is coordinated *trans* to the metalated aromatic ring and CO_3^{2-} is coordinated opposite to the cleaved C−H bond according to a concerted metalation−deprotonation (CMD)[10] mechanism. Other geometries were considered and already discussed in detail, such as proton abstraction by a *cis*-coordinated carbonate[6e,i,p] and intermolecular proton abstraction.[7,11] For the current study, only the geometry with the pseudo-*trans* relationship between CO_3^{2-} and the cleaved C−H bond was considered, in line with these previous results. To characterize the lowest TS for the C−H activation of substrate **1a** at the α and β positions, various conformations of this substrate were examined (Figure S3 in the Supporting Information). Only the geometry of each lowest-energy TS is displayed in Figure 1.[12] The lowest TS associated with the activation of a primary β C−H bond, $\mathbf{TS_{CH\beta}}$ was computed to lie 4.2 kcal mol^{-1} above $\mathbf{TS_{CH\alpha}}$. Thus, the current calculations show that the preferred site for the C−H activation of substrate **1a** is the secondary α position through $\mathbf{TS_{CH\alpha}}$. This result is consistent with the selectivity trend observed experimentally for analogous substrates bearing different alkyl groups: primary α C−H bond > secondary α C−H bond > primary β C−H bond > tertiary α C−H bond.[5b−f,6e]

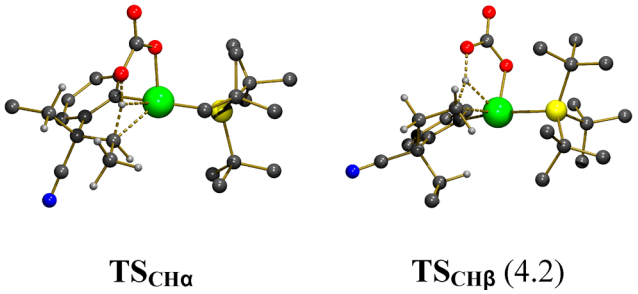

Figure 1. Geometries and relative energy (kcal mol^{-1}) of the transition-state structures computed for the C−H activation of **1a** at (left) C_α and (right) C_β.

The C−H bond activated in $\mathbf{TS_{CH\alpha}}$ presents an interaction with Pd in the reactant $\mathbf{R_{CH}}$ prior to its cleavage (Pd···H = 2.116 Å, C−H = 1.112 Å, Pd···C_α = 3.073 Å; Figure 2). In the transition-state geometry, the C−H bond is significantly elongated (1.428 Å), while the formation of the O−H bond is well-advanced (1.276 Å). This is accompanied by a significant reduction of the Pd···C_α bond distance (2.462 Å) and by the creation of an agostic interaction with the geminal C−H bond (C−H = 1.105 Å, Pd−C−H = 74.2°). Overall, this pattern of interactions leads to a relatively low activation barrier of $\Delta G^{\ddagger}$ = 19.8 kcal mol^{-1} for the C−H activation from $\mathbf{R_{CH}}$ through $\mathbf{TS_{CH\alpha}}$. This transformation is computed to be exoergic by ΔG = −19.2 kcal mol^{-1}. The product of the C−H activation step, $\mathbf{P_{CH}}$, features a five-membered palladacycle coordinated to the protonated base HCO_3^- (Figure 2, top right). The formation of BCB **2a** through C−C coupling requires dissociation of HCO_3^- to generate the ML_3 intermediate $\mathbf{R_{CC}}$. This transformation is computed to be exoergic by ΔG = −12.8 kcal mol^{-1}. A large part of this value is due to entropic effects, as the dissociation enthalpy is computed to be positive (ΔH = 4.1 kcal mol^{-1}). From $\mathbf{R_{CC}}$, the reductive C−C coupling through $\mathbf{TS_{CC}}$ was computed to have an activation barrier of $\Delta G^{\ddagger}$ = 27.4 kcal mol^{-1} and leads to the exoergic formation (ΔG = −1.9 kcal mol^{-1}) of $\mathbf{P_{CC}}$, i.e., the BCB product **2a** (presumed major diastereoisomer) coordinated to Pd[P(*t*-Bu)$_3$]. This high kinetic barrier reflects the significant ring strain that must be overcome to form the BCB system. Overall, the highest Gibbs energy barrier to overcome in the formation of **2a** from **1a** is thus $\Delta G^{\ddagger}$ = 27.4 kcal mol^{-1} associated with C−C bond formation.

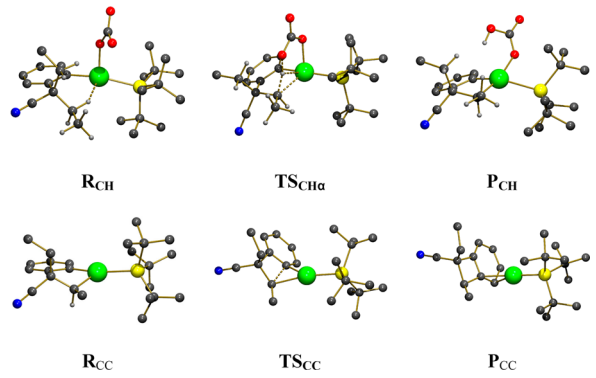

Figure 2. Geometries of the extrema along the pathway for the formation of BCB **2a** from **1a**. Most of the H atoms have been omitted for clarity.

Another possibility from $\mathbf{P_{CH}}$ is to use the proton on the coordinated HCO_3^- to break the Pd−C(sp^2) bond between the aromatic ring and the metal.[5d] The corresponding TS, $\mathbf{TS_{transf}}$ (Figure 3), was located at $\Delta G^{\ddagger}$ = 24.3 kcal mol^{-1} above $\mathbf{P_{CH}}$. In the TS, the Pd−C(sp^2) bond distance has increased to 2.251 Å (vs 1.989 Å in $\mathbf{P_{CH}}$) and the O−H bond has lengthened to 1.338 Å (vs 0.975 Å in $\mathbf{P_{CH}}$). The forming C(sp^2)−H bond has a similar length in the TS (1.332 Å) as the breaking O−H bond. From $\mathbf{P_{CH}}$, the protonation of the aromatic ring is significantly easier than the protonation of the Pd−C(sp^3) bond to revert to $\mathbf{R_{CH}}$, with the latter having an associated activation energy barrier of $\Delta G^{\ddagger}$ = 39.0 kcal mol^{-1}. The product of the protonation of the Pd−C(sp^2) bond, $\mathbf{P_{transf}}$,

dx.doi.org/10.1021/jo501610x | J. Org. Chem. 2014, 79, 11903−11910

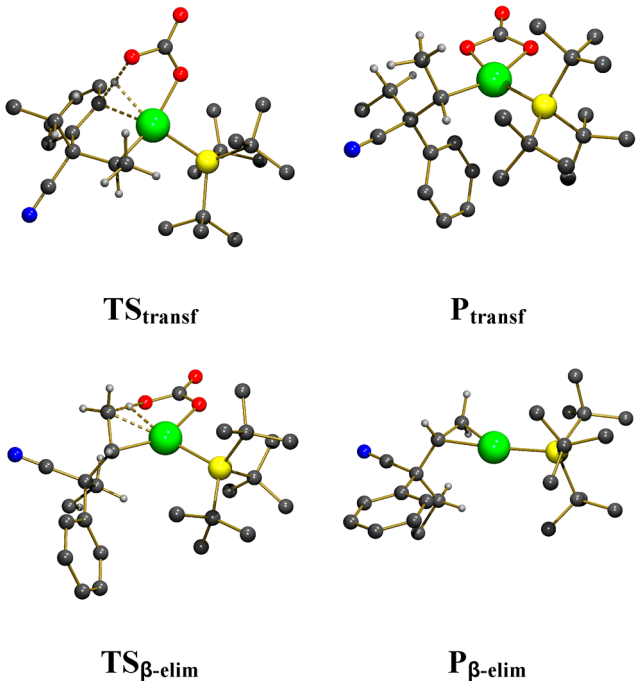

Figure 3. Geometries of the extrema along the pathway for the formation of olefin **4a** from **1a**. Most of the H atoms have been omitted for clarity.

features a κ^2-CO_3 ligand and is ΔG = −7.8 kcal mol^{-1} more stable than $\mathbf{P_{CH}}$. Rotation around the Pd−C(sp^3) bond in $\mathbf{P_{transf}}$ and concomitant decoordination of one oxygen atom of CO_3^{2-} allows the system to reach the transition-state structure $\mathbf{TS_{\beta\text{-elim}}}$ in which a β C−H bond is broken. However, the hydrogen atom is not transferred to the metal as in a typical β-H elimination. Instead, the carbonate is once again used as an internal base to deprotonate the C−H bond. In $\mathbf{TS_{\beta\text{-elim}}}$, the C−H bond has lengthened to 1.254 Å, whereas the O···H bond distance is 1.573 Å. The activation barrier for the process from $\mathbf{P_{transf}}$ to $\mathbf{TS_{\beta\text{-elim}}}$ is computed to be $\Delta G^{\ddagger}$ = 28.6 kcal mol^{-1}. The product of the transformation, $\mathbf{P_{\beta\text{-elim}}}$, features, after dissociation of HCO_3^-, olefin **4a** coordinated through the alkene C═C bond. This product is ΔG = −14.9 kcal mol^{-1} more stable than $\mathbf{P_{transf}}$, and the overall transformation from $\mathbf{P_{CH}}$ to $\mathbf{P_{\beta\text{-elim}}}$ is thus composed of two consecutive exoergic steps. $\mathbf{P_{\beta\text{-elim}}}$ is computed to be more stable than $\mathbf{P_{CC}}$ by ΔG = −7.9 kcal mol^{-1}. The olefin complex is thus the thermodynamic product.

Figure 4 shows the energy diagram for the formation of BCB **2a** and olefin **4a** from the common palladacycle intermediate $\mathbf{P_{CH}}$. The highest activation barrier to overcome along the pathway associated with the formation of $\mathbf{P_{\beta\text{-elim}}}$ is 28.6 kcal mol^{-1}, which is slightly higher than the corresponding value for the formation of the BCB product (27.4 kcal mol^{-1}). This would tend to indicate that the BCB product **2a** should be the major kinetic product of the reaction. However, a critical aspect of the mechanism is the competition between dissociation of HCO_3^- from $\mathbf{P_{CH}}$, opening the pathway toward BCB formation, and protonation of the aryl ligand, opening the pathway for olefin formation. Such dissociation processes are very difficult to compute accurately.

To address this issue, the reaction rate was simulated. The kinetic model shown in Figure 5 was considered, in which the rate constants k_i were estimated at T = 413 K using the Eyring equation with the computed $\Delta G^{\ddagger}$ values. The rate constant k_{-1} for the coordination of HCO_3^- to $\mathbf{R_{CC}}$ was approximated using the Gibbs free energy difference between $\mathbf{R_{CC}}$ and $\mathbf{P_{CH}}$, i.e., $\Delta G^{\ddagger}_{-1} = G(\mathbf{P_{CH}}) - G(\mathbf{R_{CC}}) - G(HCO_3^-)$ = 12.8 kcal mol^{-1}.

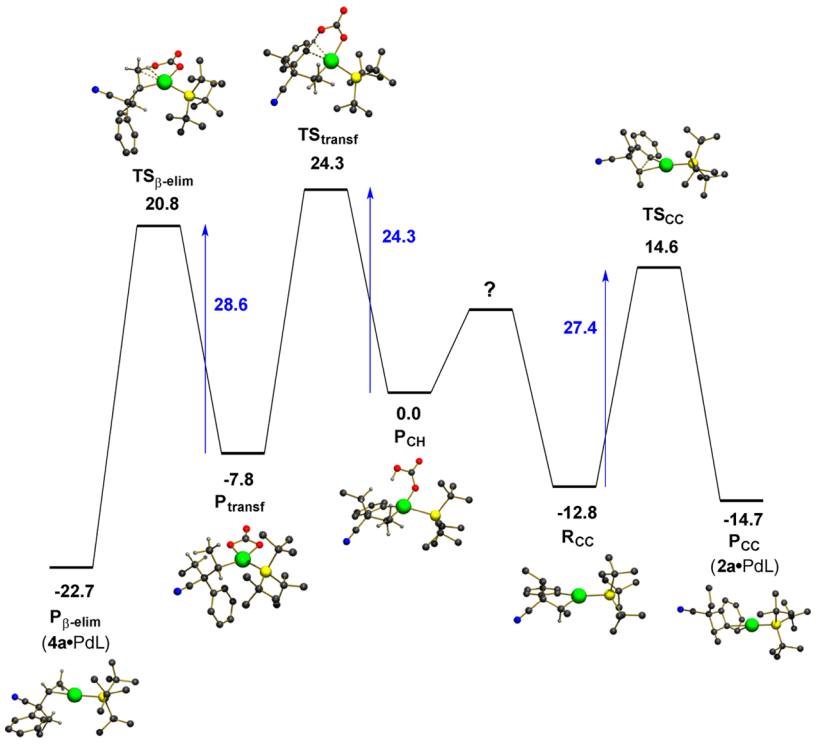

Figure 4. Comparison of the energetics (Gibbs energies, kcal mol^{-1}) associated with the pathways for C−C bond formation (right) and olefin formation (left) for substrate **1a** from palladacycle $\mathbf{P_{CH}}$.

dx.doi.org/10.1021/jo501610x | J. Org. Chem. 2014, 79, 11903−11910

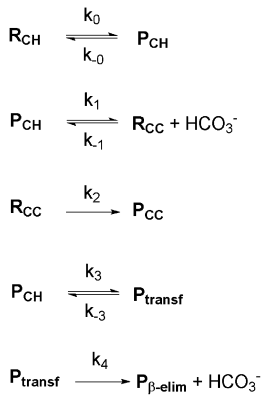

Figure 5. Kinetic model used to model the competition between the formation of benzocyclobutene **2a** and olefin **4a**.

Then the influence of different values of k_1 on the overall reaction kinetics was analyzed using this model.

The differential equations associated with the kinetic model in Figure 5 were solved using the Copasi software for an initial $\mathbf{R_{CH}}$ concentration of 1 mmol mL^{-1}.[13] Three different situations were considered, each associated with a different value of the activation barrier for the dissociation of HCO_3^- from $\mathbf{P_{CH}}$. Figure 6 shows a comparison of the evolutions of the

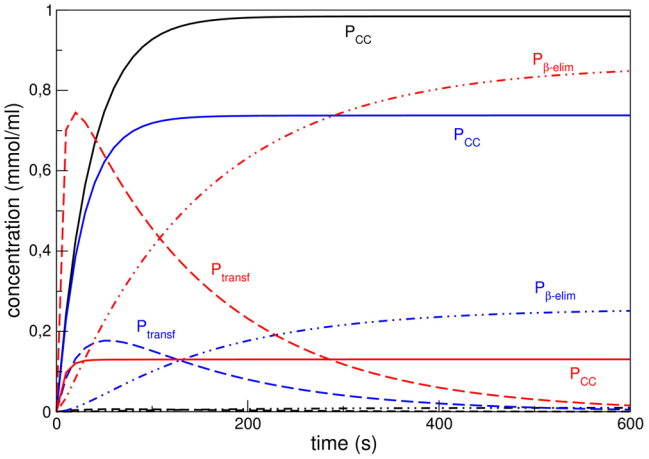

Figure 6. Comparison of the evolutions of the concentrations of $\mathbf{P_{CC}}$, $\mathbf{P_{trans}}$, and $\mathbf{P_{\beta\text{-elim}}}$ with time obtained with the kinetic model in Figure 5 using the Copasi software. The curves are associated with different values of the activation barrier for HCO_3^- dissociation from $\mathbf{P_{CH}}$ (black, 6 kcal mol^{-1}; blue, 9 kcal mol^{-1}; red, 12 kcal mol^{-1}).

concentrations of $\mathbf{P_{CC}}$, $\mathbf{P_{transf}}$, and $\mathbf{P_{\beta\text{-elim}}}$ as functions of time for the three different situations considered. The curves in black correspond to a barrier of 6 kcal mol^{-1} for HCO_3^- dissociation, and in that case, only the BCB product **2a** is formed. Increasing the barrier for dissociation to 9 kcal mol^{-1} significantly alters the final ratio between the different products, as illustrated by the curves in blue, which show that olefin **4a** is formed in a ratio of ca. 1:4 with respect to BCB **2a**. Finally, for a dissociation barrier of 12 kcal mol^{-1} (curves in red), the olefin now becomes the preferred product with a ratio qualitatively similar to the one observed experimentally. For the three situations described above, the dissociation of HCO_3^- is always much faster than protonation of the aryl ring, as the ratio k_1/k_3 varies from ca. 10^9 to 10^6. Thus, even when dissociation of HCO_3^- is ca. 10^6 times faster than protonation, the olefin formation is favored because both transformations $\mathbf{P_{CH}} \rightarrow \mathbf{P_{transf}}$ and $\mathbf{P_{transf}} \rightarrow \mathbf{P_{\beta\text{-elim}}}$ are strongly exoergic. The inverse reactions are associated with high barriers, and if HCO_3^- dissociation from $\mathbf{P_{CH}}$ is slow enough, $\mathbf{P_{transf}}$ starts to accumulate to finally yield the olefin as the major product.

It is noteworthy that the above mechanism proposed for the formation of olefin **4a** contrasts with the mechanism usually proposed for the Heck reaction, which involves β-hydride elimination to form a Pd–H bond.[14] From $\mathbf{P_{transf}}$, dissociation of CO_3^{2-} would afford an intermediate, $\mathbf{P'_{transf}}$, that might be prone to β-H elimination (Figure 7). However, in the present

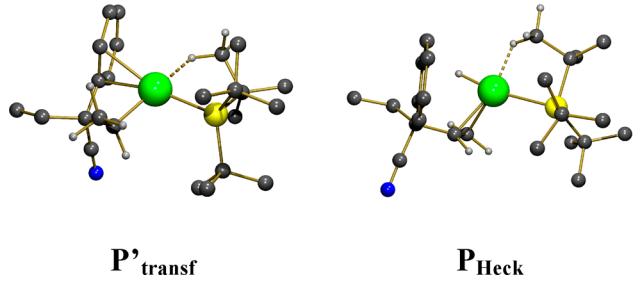

Figure 7. Geometries of $\mathbf{P'_{transf}}$ and $\mathbf{P_{Heck}}$.

case, η^2 coordination of the aromatic ring to the cationic metal center is observed, and no transition state for β-H elimination could be located. Nevertheless, the corresponding product featuring a Pd–H bond, $\mathbf{P_{Heck}}$, was located on the potential energy surface. This intermediate was computed to be less stable than $\mathbf{P'_{transf}}$ by ΔG = 10.8 kcal mol^{-1}, but more importantly, the energy difference between $\mathbf{P_{Heck}}$ and the κ^2-CO_3 intermediate $\mathbf{P_{transf}}$ is very high (ΔG = 58.7 kcal mol^{-1}). This rules out any Heck-type pathway in the formation of olefin **4a**. The proposed pathway for the formation of **4a** might also be operative in Heck reactions mediated by carbonate or similar bases. The base would substitute the X^- anion in the coordination sphere of the metal and would perform the β C–H bond cleavage similar to the current mechanism.[15]

CONCLUSION

In this article, we have analyzed the mechanism as well as the selectivity pattern for the Pd^0-catalyzed C(sp^3)–H activation of a prototypical substrate (**1a**) bearing two ethyl groups. This reaction mainly gives rise to an alkene product (**4a**) when Pd/P(*t*-Bu)$_3$ is used as the catalytic system, together with minor amounts of BCB products (**2a** and **2b**). The C–H activation step was computed to be favored for the secondary position α to the benzylic carbon over the primary position β to the benzylic carbon by more than 4 kcal mol^{-1}, in line with previous selectivity trends on analogous substrates. The corresponding five-membered palladacycle may then follow two different pathways, which were computationally characterized: (1) decoordination of the protonated base and reductive elimination to give the BCB product (**2a**) and (2) proton transfer to the aryl ligand and base-mediated β-H elimination to give the olefin product (**4a**). The results of experiments conducted using deuterated substrates were in accordance with this mechanism. The computed activation barriers would tend to suggest that BCBs **2a** and **2b** rather than olefin **4a** should be the main reaction products. However, a kinetic model showed the critical influence of the kinetics of dissociation of HCO_3^- formed after the C–H activation step in actually directing the reaction toward either of the two

dx.doi.org/10.1021/jo501610x | J. Org. Chem. 2014, 79, 11903–11910

pathways. Overall, this study addressing the formation of olefin versus carbocyclic products fills the gap of previous mechanistic reports on Pd^0-catalyzed $C(sp^3)$−H activation. In addition, it presents a new scenario for the β-hydrogen elimination mechanism in Heck-type reactions.

EXPERIMENTAL SECTION

General Information. Unless otherwise noted, all nonaqueous reactions were performed under an oxygen-free atmosphere of argon with rigid exclusion of moisture from reagents and glassware using standard techniques for manipulating air-sensitive compounds. K_2CO_3 was dried under vacuum at 140 °C for 24 h and then stored under an argon atmosphere in a glovebox. Other reagents were commercially available and were used without further purification unless otherwise stated. The solvents were dried by standard methods prior to use. Anhydrous THF was obtained by distillation over sodium/benzophenone. Analytical thin-layer chromatography (TLC) was performed using 0.25 mm silica gel 60-F plates. Visualization of the developed chromatograms was performed by UV absorbance (254 nm). Flash chromatography was performed using silica gel 60 (60−200 mesh) with the indicated solvent system according to standard techniques. GC analyses were performed with a GC−MS apparatus, with injection on a DB-5 ms column lined with a mass (EI) detection system. Infrared data are reported in reciprocal centimeters (cm^{-1}). NMR spectra (^1H, ^2H, ^{13}C, ^{19}F, DEPT 135, COSY, HMQC, NOESY) were recorded in deuterated chloroform (^1H 7.26 ppm, ^{13}C 77.0 ppm), unless otherwise noted. All spectra were obtained with complete proton decoupling. Chemical shifts are reported in parts per million (ppm). The data are reported as follows: chemical shift (multiplicity, coupling constant in Hz, integration). Multiplicities are abbreviated as follows: s = singlet, d = doublet, t = triplet, q = quartet, quint = quintet, sept = septet, m = multiplet, and br = broad. When ambiguous, proton and carbon assignments were established using COSY, HMQC, and DEPT experiments. High-resolution mass spectrometry (HRMS) was performed in electron impact (EI) mode using a magnetic analyzer.

General C−H Activation Procedure. A dry Schlenk tube containing a magnetic rod was charged with the aryl bromide, $Pd(OAc)_2$ (10 mol %), $P(t\text{-}Bu)_3{\cdot}HBF_4$ (20 mol %), and dry K_2CO_3 (1.3 equiv). The Schlenk tube was evacuated, backfilled with argon twice, and then capped with a rubber septum. Dry DMF (c = 0.24 mol L^{-1}) was injected under argon, and then the septum was replaced by a screwcap and the mixture was stirred at 140 °C (preheated oil bath) until disappearance of the starting material as monitored by GC−MS analysis. After cooling, the mixture was diluted with Et_2O and filtered through Celite. The organic solution was washed three times with brine and dried over $MgSO_4$. After filtration, the solvent was evaporated under reduced pressure. The residue was purified by flash chromatography (silica gel).

2-Ethyl-2-phenylbut-3-enenitrile (4a).[5b] Compound **4a** was obtained according to the general C−H activation procedure from 2-(2-bromophenyl)-2-ethylbutyronitrile (**1a**) (100 mg, 0.39 mmol), $Pd(OAc)_2$ (8.9 mg, 0.039 mmol, 10 mol %), $P(t\text{-}Bu)_3{\cdot}HBF_4$ (23.0 mg, 0.079 mmol, 20 mol %), and dry K_2CO_3 (71.1 mg, 0.51 mmol, 1.3 equiv). The residue was purified by flash chromatography (cyclohexane/ethyl acetate 99:1) to afford the title compound as a yellow oil (43 mg, 0.25 mmol, 64%). R_f 0.48 (cyclohexane/ethyl acetate 9:1). ^1H NMR (300 MHz, $CDCl_3$) δ 7.45−7.28 (m, 5H), 5.92 (dd, J = 17.1, 10.2 Hz, 1H), 5.54 (d, J = 17.1 Hz, 1H), 5.33 (d, J = 10.2 Hz, 1H), 2.17−1.98 (m, 2H), 1.02 (t, J = 7.3 Hz, 3H).

2-(2-Bromophenyl)-2-(1,1,2,2,2-d_5-ethyl)-3,3,4,4,4-d_5-butyronitrile (1b). LiHMDS (1.06 M in THF, 2.89 mL, 3.06 mmol) was added dropwise at 0 °C to a solution of (2-bromophenyl)acetonitrile (200 mg, 1.02 mmol) in THF (1 mL). The reaction mixture was stirred at 0 °C for 30 min, and then iodoethane-d_5 (245 μL, 3.06 mmol) was added dropwise. The reaction was stirred at rt overnight. After hydrolysis with a saturated aqueous solution of NH_4Cl (10 mL), the aqueous phase was extracted with Et_2O (3 × 5 mL), and the combined organic layers were washed with brine and dried over $MgSO_4$. Evaporation of the solvent and purification of the residue by flash chromatography (cyclohexane/ethyl acetate 95:5) afforded the title compound as a yellow oil (240 mg, 0.92 mmol, 90%). R_f 0.53 (cyclohexane/ethyl acetate 9:1). ^1H NMR (300 MHz, $CDCl_3$) δ 7.69 (dd, J = 7.9, 1.6 Hz, 1H), 7.61 (dd, J = 7.9, 1.3 Hz, 1H), 7.36−7.30 (m, 1H), 7.19−7.14 (m, 1H). $^{13}C\{^1H\}$ NMR (75 MHz, $CDCl_3$) δ 141.6, 140.3, 137.3, 134.9, 133.2, 128.1, 126.0, 57.4, 34.6 (quint, J = 19 Hz), 14.4 (sept, J = 19 Hz). IR (neat) ν 2970, 2224, 1564, 1469 cm^{-1}. HRMS (EI) calcd for $C_{12}H_4D_{10}BrN$ [$M^{+\bullet}$] 261.0937, found 261.0932.

2-(1,1,2,2,2-d_5-Ethyl)-2-phenyl-3,4,4-d_3-but-3-enenitrile (4b). Compound **4b** was obtained according to the general C−H activation procedure from compound **1b** (50 mg, 0.19 mmol), $Pd(OAc)_2$ (4.4 mg, 0.02 mmol, 10 mol %), $P(t\text{-}Bu)_3{\cdot}HBF_4$ (11.2 mg, 0.038 mmol, 20 mol %), and dry K_2CO_3 (34.8 mg, 0.25 mmol, 1.3 equiv). The residue was purified by flash chromatography (cyclohexane/ethyl acetate 98:2) to afford the title compound as a yellow oil (17 mg, 0.10 mmol, 53%). R_f 0.50 (cyclohexane/ethyl acetate 9:1). Compound **4b** was obtained with 71% deuterium incorporation on the aromatic ring as determined by ^2H NMR spectroscopy (acetone/acetone-d_6 95:5). ^1H NMR (300 MHz, $CDCl_3$) δ 7.45−7.29 (m, 5H). $^{13}C\{^1H\}$ NMR (75 MHz, $CDCl_3$) δ 138.7, 137.0 (t, J = 24.8 Hz), 129.0, 128.0, 126.2, 120.7, 115.8 (quint, J = 24.2 Hz), 50.9, 31.6−32.7 (m), 9.2−8.2 (m). IR (neat) ν 2970, 2230, 1574, 1470 cm^{-1}. HRMS (EI) calcd for $C_{12}H_5D_8N$ [$M^{+\bullet}$] 179.1545, found 179.1543.

2-(2-Bromophenyl)-2-(2,2,2-d_3-ethyl)-4,4,4-d_3-butyronitrile (1c). LiHMDS (1.06 M in THF, 2.89 mL, 3.06 mmol) was added dropwise at 0 °C to a solution of (2-bromophenyl)acetonitrile (200 mg, 1.02 mmol) in THF (1 mL). The reaction mixture was stirred at 0 °C for 30 min, and then iodoethane-2,2,2-d_3 (245 μL, 3.06 mmol) was added dropwise. The reaction mixture was stirred at rt overnight. After hydrolysis with a saturated aqueous solution of NH_4Cl (10 mL), the aqueous phase was extracted with Et_2O (3 × 5 mL), and the combined organic layers were washed with brine and dried over $MgSO_4$. Evaporation of the solvent and purification of the residue by flash chromatography (cyclohexane/ethyl acetate 95:5) afforded the title compound as a yellow oil (228 mg, 0.88 mmol, 86%). R_f 0.50 (cyclohexane/ethyl acetate 9:1). ^1H NMR (300 MHz, $CDCl_3$) δ 7.68 (dd, J = 7.9, 1.6 Hz, 1H), 7.60 (dd, J = 7.9, 1.3 Hz, 1H), 7.35−7.29 (m, 1H), 7.18−7.13 (m, 1H), 2.61 (d, J = 14.1 Hz, 1H), 2.04 (d, J = 14.1 Hz, 1H). $^{13}C\{^1H\}$ NMR (75 MHz, $CDCl_3$) δ 135.9, 134.6, 131.6, 129.2, 127.5, 122.4, 120.2, 52.0, 29.7, 9.0 (sept, J = 19 Hz). IR (neat) ν 2228, 1560, 1471, 1018 cm^{-1}. HRMS (EI) calcd for $C_{12}H_8D_6BrN$ [$M^{+\bullet}$] 257.0686, found 257.0689.

2-(2,2,2-d_3-Ethyl)-2-phenyl-4,4-d_2-but-3-enenitrile (4c). Compound **4c** was obtained according to the general C−H activation procedure from compound **1c** (50 mg, 0.19 mmol), $Pd(OAc)_2$ (4.4 mg, 0.02 mmol, 10 mol %), $P(t\text{-}Bu)_3{\cdot}HBF_4$ (11.2 mg, 0.038 mmol, 20 mol %), and dry K_2CO_3 (34.8 mg, 0.25 mmol, 1.3 equiv). The residue was purified by flash chromatography (cyclohexane/ethyl acetate 98:2) to afford the title compound as a yellow oil (20 mg, 0.11 mmol, 59%). R_f 0.48 (cyclohexane/ethyl acetate 9:1). Compound **4c** showed no deuterium incorporation on the aromatic ring as determined by ^2H NMR spectroscopy (acetone/acetone-d_6 95:5). ^1H NMR (400 MHz, $CDCl_3$) δ 7.44−7.42 (m, 2H), 7.40−7.37 (m, 2H), 7.32−7.30 (m, 1H), 5.90 (s, 1H), 2.09 (d, J = 14.0 Hz, 1H), 2.02 (d, J = 14.0 Hz, 1H). $^{13}C\{^1H\}$ NMR (125 MHz, $CDCl_3$) δ 139.1, 137.7, 129.3, 128.3, 126.5, 121.0, 116.5, 51.4, 33.2, 9.1. IR (neat) ν 2227, 1590, 1493 cm^{-1}. HRMS (EI) calcd for $C_{12}H_8D_3N$ [$M^{+\bullet}$] 176.1356, found 176.1359.

2-(2-Bromophenyl)-2-(1,1-d_2-ethyl)-3,3-d_2-butyronitrile (1d). LiHMDS (1.06 M in THF, 2.89 mL, 3.06 mmol) was added dropwise at 0 °C to a solution of (2-bromophenyl)acetonitrile (200 mg, 1.02 mmol) in THF (1 mL). The reaction mixture was stirred at 0 °C for 30 min, and then iodoethane-1,1-d_2 (245 μL, 3.06 mmol) was added dropwise. The reaction mixture was stirred at rt overnight. After hydrolysis with a saturated aqueous solution of NH_4Cl (10 mL), the aqueous phase was extracted with Et_2O (3 × 5 mL), and the combined organic layers were washed with brine and dried over $MgSO_4$. Evaporation of the solvent and purification of the residue by flash chromatography (cyclohexane/ethyl acetate 95:5) afforded the title compound as a yellow oil (239 mg, 0.93 mmol, 91%). R_f 0.48

(cyclohexane/ethyl acetate 9:1). ^{1}H NMR (300 MHz, $CDCl_3$) δ 7.68 (dd, J = 7.8, 1.5 Hz, 1H), 7.60 (dd, J = 7.8, 1.2 Hz, 1H), 7.35−7.29 (m, 1H), 7.19−7.13 (m, 1H), 0.89 (s, 6H). ^{13}C{^{1}H} NMR (75 MHz, $CDCl_3$) δ 136.3, 135.0, 132.1, 129.7, 128.0, 122.9, 120.7, 52.3, 29.6 (quint, J = 19 Hz), 10.0. IR (neat) ν 2968, 2232, 1565, 1470 cm^{-1}. HRMS (EI) calcd for $C_{12}H_{10}D_4BrN$ [$M^{+\bullet}$] 255.0561, found 255.0555.

2-(1,1-d_2-Ethyl)-2-phenyl-3-*d*-but-3-enenitrile (4d). Compound **4d** was obtained according to the general C−H activation procedure from compound **1d** (50 mg, 0.19 mmol), $Pd(OAc)_2$ (4.4 mg, 0.02 mmol, 10 mol %), P(t-Bu)$_3$·HBF$_4$ (11.3 mg, 0.039 mmol, 20 mol %), and dry K_2CO_3 (35.0 mg, 0.25 mmol, 1.3 equiv). The residue was purified by flash chromatography (cyclohexane/ethyl acetate 98:2) to afford the title compound as a yellow oil (18 mg, 0.10 mmol, 54%). R_f 0.50 (cyclohexane/ethyl acetate 9:1). Compound **4d** was obtained with 43% deuterium incorporation on the aromatic ring as determined by ^{2}H NMR spectroscopy (acetone/acetone-d_6 95:5). ^{1}H NMR (300 MHz, $CDCl_3$) δ 7.45−7.28 (m, 5H), 5.54−5.52 (m, 1H), 5.33−5.32 (m, 1H), 1.01 (s, 3H). ^{13}C{^{1}H} NMR (75 MHz, $CDCl_3$) δ 138.6, 137.0 (t, J = 24.9 Hz), 128.9, 127.9, 126.1, 120.6, 116.3, 50.9, 32.3, 9.5. IR (neat) ν 2970, 2236, 1448 cm^{-1}. HRMS (EI) calcd for $C_{12}H_{10}D_3N$ [$M^{+\bullet}$] 174.1231, found 174.1231.

Computational Details. Geometry optimizations were performed with the Gaussian 09 package at the B3PW91 level of hybrid density functional theory.[16−18] The palladium atom was represented by the relativistic effective core potential (RECP) from the Stuttgart group and the associated basis sets,[19] augmented by an f polarization function.[20] The phosphorus atom was represented by the RECP from the Stuttgart group and the associated basis set,[21] augmented by a d polarization function.[22] The remaining atoms (C, H, N, O) were represented by a 6-31G(d,p) basis set. The influence of the solvent (*N*,*N*-dimethylformamide) was taken into consideration through single-point calculations on the gas-phase optimized geometry by COSMO calculations with the SMD model using the ORCA software.[23] For the COSMO calculations, the pseudopotential was kept on Pd and all of the atoms were treated with def2-tzvp basis sets.[24] Influence of the dispersion forces was considered by adding to the COSMO energy the D3(BJ) corrections as described by Grimme.[25] All of the energies reported in the present work are Gibbs free energies obtained by summing the COSMO energy, the gas-phase Gibbs contribution at 413 K, and the D3(BJ) correction. To complement our DFT study, we computed the energies of the various extrema using other DFT methods (Tables S1 and S2 in the Supporting Information), and the results were very similar to those obtained with B3PW91; therefore, our computational strategy seems sound.

■ ASSOCIATED CONTENT

Ⓢ Supporting Information

Figures S1−S3, copies of NMR spectra for new compounds, and Cartesian coordinates for computed structures. This material is available free of charge via the Internet at http://pubs.acs.org.

■ AUTHOR INFORMATION

Corresponding Authors

*E-mail: clot@univ-montp2.fr.

*E-mail: olivier.baudoin@univ-lyon1.fr.

Notes

The authors declare no competing financial interest.

■ ACKNOWLEDGMENTS

This work was financially supported by Agence Nationale de la Recherche (programme blanc "AlCaCHA") and Institut Universitaire de France.

■ REFERENCES

(1) (a) *Handbook of C−H Transformations*; Dyker, G., Ed.; Wiley-VCH: Weinheim, Germany, 2005. (b) *C−H Activation*; Yu, J.-Q., Shi, Z., Eds.; Topics in Current Chemistry, Vol. *292*; Springer: Berlin, 2010.

(2) For selected general reviews, see: (a) Kakiuchi, F.; Chatani, N. *Adv. Synth. Catal.* **2003**, *345*, 1077. (b) Dick, A. R.; Sanford, M. S. *Tetrahedron* **2006**, *62*, 2439. (c) Godula, K.; Sames, D. *Science* **2006**, *312*, 67. (d) Davies, H. M. L.; Manning, J. R. *Nature* **2008**, *451*, 417.

(3) For selected reviews, see: (a) Campeau, L.-C.; Fagnou, K. *Chem. Commun.* **2006**, 1253. (b) Alberico, D.; Scott, M. E.; Lautens, M. *Chem. Rev.* **2007**, *107*, 174. (c) Seregin, I. V.; Gevorgyan, V. *Chem. Soc. Rev.* **2007**, *36*, 1173. (d) Chen, X.; Engle, K. M.; Wang, D.-H.; Yu, J.-Q. *Angew. Chem., Int. Ed.* **2009**, *48*, 5094. (e) Ackermann, L.; Vicente, R.; Kapdi, A. R. *Angew. Chem., Int. Ed.* **2009**, *48*, 9792. (f) Colby, D. A.; Bergman, R. G.; Ellman, J. A. *Chem. Rev.* **2010**, *110*, 624. (g) Mkhalid, I. A. I.; Barnard, J. H.; Marder, T. B.; Murphy, J. M.; Hartwig, J. F. *Chem. Rev.* **2010**, *110*, 890. (h) Lyons, T. W.; Sanford, M. S. *Chem. Rev.* **2010**, *110*, 1147. (i) Arockiam, P. B.; Bruneau, C.; Dixneuf, P. H. *Chem. Rev.* **2012**, *112*, 5879. (j) Kuhl, N.; Hopkinson, M. N.; Wencel-Delord, J.; Glorius, F. *Angew. Chem., Int. Ed.* **2012**, *51*, 10236.

(4) (a) Jazzar, R.; Hitce, J.; Renaudat, A.; Sofack-Kreutzer, J.; Baudoin, O. *Chem.—Eur. J.* **2010**, *16*, 2654. (b) Baudoin, O. *Chem. Soc. Rev.* **2011**, *40*, 4902. (c) Li, H.; Li, B.-J.; Shi, Z.-J. *Catal. Sci. Technol.* **2011**, *1*, 191. (d) Dastbaravardeh, N.; Christakakou, M.; Haider, M.; Schnürch, M. *Synthesis* **2014**, *46*, 1421.

(5) (a) Baudoin, O.; Herrbach, A.; Guéritte, F. *Angew. Chem., Int. Ed.* **2003**, *42*, 5736. (b) Hitce, J.; Retailleau, P.; Baudoin, O. *Chem.—Eur. J.* **2007**, *13*, 792. (c) Hitce, J.; Baudoin, O. *Adv. Synth. Catal.* **2007**, *349*, 2054. (d) Chaumontet, M.; Piccardi, R.; Audic, N.; Hitce, J.; Peglion, J.-L.; Clot, E.; Baudoin, O. *J. Am. Chem. Soc.* **2008**, *130*, 15157. (e) Chaumontet, M.; Piccardi, R.; Baudoin, O. *Angew. Chem., Int. Ed.* **2009**, *48*, 179. (f) Rousseaux, S.; Davi, M.; Sofack-Kreutzer, J.; Pierre, C.; Kefalidis, C. E.; Clot, E.; Fagnou, K.; Baudoin, O. *J. Am. Chem. Soc.* **2010**, *132*, 10706. (g) Pierre, C.; Baudoin, O. *Org. Lett.* **2011**, *13*, 1816. (h) Guyonnet, M.; Baudoin, O. *Org. Lett.* **2012**, *14*, 398. (i) Martin, N.; Pierre, C.; Davi, M.; Jazzar, R.; Baudoin, O. *Chem.—Eur. J.* **2012**, *18*, 4480. (j) Sofack-Kreutzer, J.; Martin, N.; Renaudat, A.; Jazzar, R.; Baudoin, O. *Angew. Chem., Int. Ed.* **2012**, *51*, 10399.

(6) For selected examples, see: (a) Dyker, G. *Angew. Chem., Int. Ed. Engl.* **1992**, *31*, 1023. (b) Catellani, M.; Motti, E.; Ghelli, S. *Chem. Commun.* **2000**, 2003. (c) Dong, C.-G.; Hu, Q.-S. *Angew. Chem., Int. Ed.* **2006**, *45*, 2289. (d) Ren, H.; Knochel, P. *Angew. Chem., Int. Ed.* **2006**, *45*, 3462. (e) Lafrance, M.; Gorelsky, S. I.; Fagnou, K. *J. Am. Chem. Soc.* **2007**, *129*, 14570. (f) Watanabe, T.; Oishi, S.; Fujii, N.; Ohno, H. *Org. Lett.* **2008**, *10*, 1759. (g) Motti, E.; Catellani, M. *Adv. Synth. Catal.* **2008**, *350*, 565. (h) Wasa, M.; Engle, K. M.; Yu, J.-Q. *J. Am. Chem. Soc.* **2009**, *131*, 9886. (i) Rousseaux, S.; Gorelsky, S. I.; Chung, B. K. W.; Fagnou, K. *J. Am. Chem. Soc.* **2010**, *132*, 10692. (j) Nakanishi, M.; Katayev, D.; Besnard, C.; Kündig, E. P. *Angew. Chem., Int. Ed.* **2011**, *50*, 7438. (k) Anas, S.; Cordi, A.; Kagan, H. B. *Chem. Commun.* **2011**, *47*, 11483. (l) Saget, T.; Lemouzy, S. J.; Cramer, N. *Angew. Chem., Int. Ed.* **2012**, *51*, 2238. (m) Tsukano, C.; Okuno, M.; Takemoto, Y. *Angew. Chem., Int. Ed.* **2012**, *51*, 2763. (n) Piou, T.; Neuville, L.; Zhu, J. *Angew. Chem., Int. Ed.* **2012**, *51*, 11561. (o) Saget, T.; Cramer, N. *Angew. Chem., Int. Ed.* **2012**, *51*, 12842. (p) Larionov, E.; Nakanishi, M.; Katayev, D.; Besnard, C.; Kündig, E. P. *Chem. Sci.* **2013**, *4*, 1995. (q) Bheeter, C. B.; Jin, R.; Bera, J. K.; Dixneuf, P. H.; Doucet, H. *Adv. Synth. Catal.* **2014**, *356*, 119. (r) Mao, J.; Zhang, S.-Q.; Shi, B.-F.; Bao, W. *Chem. Commun.* **2014**, *50*, 3692. (s) Yan, J.-X.; Li, H.; Shi, J.-L.; Wang, X.; Shi, Z.-J. *Angew. Chem., Int. Ed.* **2014**, *53*, 4945.

(7) Kefalidis, C. E.; Baudoin, O.; Clot, E. *Dalton Trans.* **2010**, *39*, 10528.

(8) The observed fragmentations of the molecular ions of **2a** and **2b** in the mass spectrum (EI) as well as the presence of two quartets resonating at ca. 3.3 ppm (methine signal) in the ^{1}H NMR spectrum

of the crude mixture are consistent with this assignment (Figure S1 in the Supporting Information).
(9) Zhao, J.; Campo, M.; Larock, R. C. *Angew. Chem., Int. Ed.* **2005**, *44*, 1873.
(10) For reviews, see: (a) Boutadla, Y.; Davies, D. L.; Macgregor, S. A.; Poblador-Bahamonde, A. I. *Dalton Trans.* **2009**, 5820. (b) Balcells, D.; Clot, E.; Eisenstein, O. *Chem. Rev.* **2010**, *110*, 749. (c) Lapointe, D.; Fagnou, K. *Chem. Lett.* **2010**, *39*, 1118. (d) Ackermann, L. *Chem. Rev.* **2011**, *111*, 1315. (e) Gorelsky, S. I. *Coord. Chem. Rev.* **2013**, *257*, 153.
(11) Engelin, C.; Jensen, T.; Rodriguez-Rodriguez, S.; Fristrup, P. *ACS Catal.* **2013**, *3*, 294.
(12) The formation of diastereoisomers **2a** and **2b** is not discussed therein because of the lack of experimental evidence on their structure and configuration.
(13) Hoops, S.; Sahle, S.; Gauges, R.; Lee, C.; Pahle, J.; Simus, N.; Singhal, M.; Xu, L.; Mendes, P.; Kummer, U. *Bioinformatics* **2006**, *22*, 3067.
(14) For selected computational studies of the Heck reaction, see: (a) Lin, B.-L.; Liu, L.; Fu, Y.; Luo, S.-W.; Chen, Q.; Guo, Q.-X. *Organometallics* **2004**, *23*, 2114. (b) Surawatanawong, P.; Fan, Y.; Hall, M. B. *J. Organomet. Chem.* **2008**, *693*, 1552. (c) Ambrogio, I.; Fabrizi, G.; Cacchi, S.; Henriksen, S. T.; Fristrup, P.; Tanner, D.; Norrby, P.-O. *Organometallics* **2008**, *27*, 3187. (d) Henriksen, S. T.; Tanner, D.; Cacchi, S.; Norrby, P.-O. *Organometallics* **2009**, *28*, 6201.
(15) For a similar mechanism proposed for the formation of allenes by a Heck-type reaction of aryl bromides with alkynes, see: Nella, N.; Parker, E.; Hitce, J.; Larini, P.; Jazzar, R.; Baudoin, O. *Chem.—Eur. J.* **2014**, DOI: 10.1002/chem.201403213.
(16) Frisch, M. J.; Trucks, G. W.; Schlegel, H. B.; Scuseria, G. E.; Robb, M. A.; Cheeseman, J. R.; Scalmani, G.; Barone, V.; Mennucci, B.; Petersson, G. A.; Nakatsuji, H.; Caricato, M.; Li, X.; Hratchian, H. P.; Izmaylov, A. F.; Bloino, J.; Zheng, G.; Sonnenberg, J. L.; Hada, M.; Ehara, M.; Toyota, K.; Fukuda, R.; Hasegawa, J.; Ishida, M.; Nakajima, T.; Honda, Y.; Kitao, O.; Nakai, H.; Vreven, T.; Montgomery, J. A., Jr.; Peralta, J. E.; Ogliaro, F.; Bearpark, M.; Heyd, J. J.; Brothers, E.; Kudin, K. N.; Staroverov, V. N.; Kobayashi, R.; Normand, J.; Raghavachari, K.; Rendell, A.; Burant, J. C.; Iyengar, S. S.; Tomasi, J.; Cossi, M.; Rega, N.; Millam, J. M.; Klene, M.; Knox, J. E.; Cross, J. B.; Bakken, V.; Adamo, C.; Jaramillo, J.; Gomperts, R.; Stratmann, R. E.; Yazyev, O.; Austin, A. J.; Cammi, R.; Pomelli, C.; Ochterski, J. W.; Martin, R. L.; Morokuma, K.; Zakrzewski, V. G.; Voth, G. A.; Salvador, P.; Dannenberg, J. J.; Dapprich, S.; Daniels, A. D.; Farkas, Ö.; Foresman, J. B.; Ortiz, J. V.; Cioslowski, J.; Fox, D. J. *Gaussian 09*, revision B.01; Gaussian, Inc.: Wallingford, CT, 2009
(17) Becke, A. D. *J. Chem. Phys.* **1993**, *98*, 5648.
(18) Perdew, J. P.; Wang, Y. *Phys. Rev. B* **1992**, *45*, 13244.
(19) Andrae, D.; Häußermann, U.; Dolg, M.; Stoll, H.; Preuß, H. *Theor. Chim. Acta* **1990**, *77*, 123.
(20) Ehlers, A. W.; Böhme, M.; Dapprich, S.; Gobbi, A.; Höllwarth, A.; Jonas, V.; Köhler, K. F.; Stegmann, R.; Veldkamp, A.; Frenking, G. *Chem. Phys. Lett.* **1993**, *208*, 111.
(21) Bergner, A.; Dolg, M.; Küchle, W.; Stoll, H.; Preuß, H. *Mol. Phys.* **1993**, *80*, 1431.
(22) Höllwarth, A.; Böhme, M.; Dapprich, S.; Ehlers, A. W.; Gobbi, A.; Jonas, V.; Köhler, K. F.; Stegmann, R.; Veldkamp, A.; Frenking, G. *Chem. Phys. Lett.* **1993**, *208*, 237.
(23) (a) COSMO: Klamt, A. *Wiley Interdiscip. Rev.: Comput. Mol. Sci.* **2009**, *1*, 699. (b) SMD model: Marenich, A. V.; Cramer, C. J.; Truhlar, D. G. *J. Phys. Chem. B* **2009**, *113*, 6378. (c) ORCA, version 3.0.2: Neese, F. *Wiley Interdiscip. Rev.: Comput. Mol. Sci.* **2012**, *2*, 73.
(24) Weigend, F.; Ahlrichs, R. *Phys. Chem. Chem. Phys.* **2005**, *7*, 3297.
(25) (a) Grimme, S.; Ehrlich, S.; Goerigk, L. *J. Comput. Chem.* **2011**, *32*, 1456. (b) Grimme, S.; Antony, J.; Ehrlich, S.; Krieg, H. *J. Chem. Phys.* **2010**, *132*, No. 154104.